Numerical Analysis of Effect of Pitch Angle on a Small Scale Vertical Axis Wind Turbine

Bose Sumantraa R., Chandramouli S., Premsai T. P., Prithviraj P.,
Vivek M., V. Ratna Kishore[‡]

Department of Mechanical Engineering, Amrita School of Engineering, Ettimadai Campus
Amrita Vishwa Vidyapeetham, Coimbatore, India

(bose.sumantraa@gmail.com, ajayaant93@gmail.com, premsai7736@gmail.com, Prithvi28@ymail.com,
vivekmugundhan@gmail.com, ratnavk@gmail.com)

[‡] Corresponding Author; V. Ratna Kishore, Department of Mechanical Engineering, Amrita School of Engineering,
Ettimadai Campus, Amrita Vishwa Vidyapeetham, Coimbatore, India, Tel: +91 812 295 7821
Fax: +91 422 265 6274, ratnavk@gmail.com

Abstract- The current work involves a numerical study of the effect of preset pitch angle on the performance of a Vertical Axis Wind Turbine (VAWT). A three bladed H-Darrieus VAWT has been considered for the study. The equations governing the flow are solved using a commercial CFD code ANSYS CFX 13. The turbine with NACA 0015 profile and zero pitch angle is taken as the reference case for comparison. The analysis has been done for three pitch angles -6°, 0°, +6°, tip speed ratios (TSR) from 1 to 2.2 and wind velocities of 6, 8 and 10 m/s. Of the pitch angle considered, the best performance is observed with -6° for all tip speed ratios and wind velocities. This has been explained by studying the instantaneous torque characteristics of the turbine. It is seen that at any given instant, the blade in the upwind region contributes significantly to the positive torque with other blades either contributing less or negating the positive torque. The pressure coefficient distributions over the upwind blade and stream lines at different azimuthal angles have also been analysed to understand the effect of pitch.

Keywords: VAWT, Pitch angle, Power coefficient, CFD

1. Introduction

Over the last decade, Vertical Axis Wind Turbines (VAWTs) have gained staggering interest against their counterparts. One of the main advantages of VAWTs over the Horizontal Axis Wind Turbines (HAWTs) is that it does not require any yawing mechanism to align it along the wind direction for its operation. This makes it suitable for power generation at small scales in urban areas where wind magnitude and direction are highly fluctuating due to the presence of tall buildings and other structures. Also, they operate at relatively low operational speeds and thus they are less noisy. The complex flow phenomena associated with the VAWT make their performance predictions difficult. Due to this, performance predictions using simplified analytical methods like BEM are not so accurate. Detailed CFD flow calculations are required to predict turbine performance more realistically [1]. One of the major deficiencies of this turbine is its inability to self start at low wind speeds. To overcome this deficiency one method adopted is the pitch control as reported by Lazauskas [2]. Recent studies have showed that a variable pitch control strategy based on the operating conditions can improve the starting torque and performance characteristics of the turbine [3].

Aslam et al. [1] reviewed various configurations of VAWT and the design techniques employed for the design of VAWT. They concluded that VAWT can be used in power production in the range 2 kW to 4 MW with reasonable payback period and is suitable for integration with tall buildings where wind velocities are greater than 14 m/s. They found that for different configurations, desirable coefficient of power C_p is obtained for different ranges of tip speed ratios (λ). They suggested CFD is capable of predicting performance with higher degree of accuracy and can reduce time and cost involved in their design. There have been several experimental and numerical studies on effect of pitch angle on the performance of VAWT which have been detailed below. Initially, experimental studies are presented, followed by studies done numerically and then literature on studied involving both numerical and experimental work are presented.

Lazauskas [2] developed a mathematical model to study three difference mechanisms for pitch control of VAWTs and their performance. They concluded that these mechanisms can be optimized for better starting torque, broader operating range and greater efficiency as compared to the fixed pitch blades. Fiedler et al. [4] investigated the effects of toe in, toe out pitch angles and blade mount point location offset on 2.5

m diameter, 3 m high, high solidity three bladed VAWT by conducting experiments in an open-air wind tunnel. The blades were of NACA 0015 profile with chord length of 0.4m. It was observed that a blade with toe out pitch improved the performance by 29% while a toe in pitch decreased the performance by 47% with respect to the zero pitch case. It was also seen that the turbine showed low power output as the blade mount point shifted towards the leading edge due to the inherent toe in pitch.

Klimas [5] developed schemes (SIMOS, DARTER and PAREP) for predicting the aerodynamic efficiency of VAWT and they in general were compared with wind tunnel experiments conducted in Sandia National Laboratories. They suggested that the choice of scheme is to be based on the intended application. Nobile et al. [6] performed CFD analysis to predict the dynamics stall in VAWT at low λ (<5). A 2D study was done on a three bladed VAWT with NACA0018 profile using different RANS turbulence model. It was concluded that SST model predicted well as compared to other models. Qin et al. [7] numerically studied a rooftop size H type straight bladed VAWT. They solved 2D and 3D unsteady flow fields by solving URANS using sliding mesh techniques in FLUENT. They observed stall and strong interactions of blade wakes with the following blades. They concluded that the presence of three dimensional effects make 3D analysis important for realistic predictions. Chen and Kuo [8] numerically studied the effect of pitch angle and blade camber on the flow characteristics and performance of a small size Darrieus VAWT for a uniform wind velocity of 10 m/s. The study was done for three cambers (NACA0012, 2412 and 4412) and pitch angle varying from -10° to 10°. They found that the initial acceleration to be the highest at pitch -10° and monotonously decreases with increase in the pitch angle. For a fixed pitch, the blade with larger camber (NACA 4412) had better self starting characteristics.

Howell et al. [9] performed experimental and computational study on aerodynamics and performance of a small scale VAWT. Wind tunnel experiments were done to validate the results obtained from 2D and 3D unsteady CFD model predictions. It was seen that the performance of the turbine degrades with smooth surface up to a critical Reynolds number of 30,000 and is enhanced by a smooth surface finish above this critical value. Both two bladed and three bladed rotors were tested and a significant increase in performance coefficient is observed for the three bladed rotors over large operating range. The change in pitch angle affects the dynamic stall behaviour of the turbine and thus affects the performance of the turbine. The CFD studies showed that the 2D model over-predicted coefficient of performance as compared to those obtained from 3D models and experiments. The presence of tip vortices makes 3D predictions to be more close to experiments than 2D predictions. Erickson et al. [10] experimentally characterized the effects of sinusoidal pitch actuation on the operability and efficiency of a high solidity VAWT in a wind tunnel using a cam mechanism to control pitch over a wide range of design and operational conditions. They concluded that a tuned first order sinusoidal actuation system achieved a maximum absolute efficiency of 43.6% which was 35%

above the fixed blade reference configuration and improved performance even at conditions other than optimal. It was concluded that a low order 2D theoretical model can accurately predict the trends and maximum efficiency of the system. Miau et al. [3] performed both experimental and numerical studies focused on improving the starting torque of a small VAWT at low tip speed ratios using variable pitch. The study was done on a three straight bladed turbine with NACA0015 profile of chord length 0.090 m, diameter 0.9 m and height 0.54 m. It was found that in the variable pitch mode, β= -70° to +70° recorded high performance for λ of 0 to 2 as against β= -10° to +10°. Both numerical and experimental studies showed that variable pitch control strategy is better than fixed pitch control. Sabaeifard et al. [11] numerically and experimentally studied the aerodynamics and performance of a small scale Darrieus-type straight-bladed vertical axis wind turbines at different λ. The CFD study was done using a 2D model with moving reference frame and RNG k-ε model. The maximum power coefficient was obtained to be 0.36 and 0.32 at λ=3.5 by numerical and experimental analysis respectively. Benedict et al. [12] conducted numerical and experimental studies on the effect of pitch angle on the performance of VAWT at Reynolds number of 40,000. They built a simplified blade pitch changing mechanism and tested the turbine in a wind tunnel. The 2D CFD model developed compared well with their experimental data. They observed that the turbine efficiency was highest when the pitching amplitude was between ±20° to ±25°. The optimum λ where the maximum power was extracted decreased with increase in pitch amplitude. The power is extracted in the frontal half of rotation and then lost in the rear half due large virtual camber and incidence induced by flow curvatures. It was concluded that the performance of a fixed-pitch turbine could be enhanced by reducing the pitch angle and chord/radius ratio, or by using cambered blades.

Based on the literature survey done, it is seen that the effect of pitch on the performance of VAWT has not been studied at low wind velocities (<10 m/s). The objective of the current work is to numerically study, the effect of preset pitch angle on the performance of a VAWT for three different pitch angles -6°, 0°, +6° for tip speed ratios of 1, 1.2, 1.4, 1.6, 1.8, 2 and 2.2 and low wind velocities of 6, 8 and 10 m/s. The relevant parameters in the study are (1) tip speed ratio ($\lambda = r\omega/U_\infty$, where, r is the radius of the turbine, ω is the angular velocity and U_∞ is the free stream velocity of wind); and (2) coefficient of power ($C_p = \tau\omega/0.5\rho dh U_\infty^3$, where, τ is the average torque produced by the turbine, ρ is the density of air, d, h are the diameter and height of the turbine). Coefficient of power is the ratio of the power generated by the turbine to the power contained in the wind.

2. Mathematical Model and Solution Methodology

2.1 Governing equations

Since the flow velocities in the domain are much smaller than sound velocity, the flow is treated as incompressible.

Since the flow is unsteady and turbulent, Unsteady Reynolds Averaged Navier Stokes (URANS) equations are solved with SST k-ω turbulence model [13].

(a)

(b)
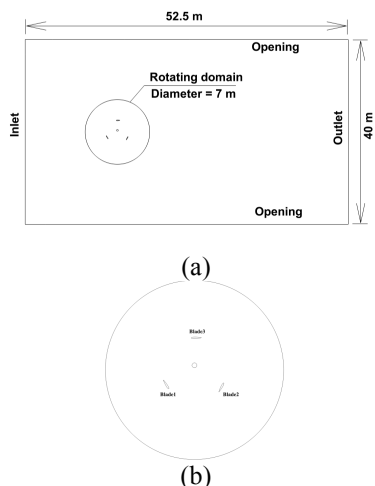
Fig. 1 (a) Computational domain (b) Rotating domain

2.2 Computational domain and mesh generation

The 2D domain considered for analysis is shown in Fig. 1(a). The domain considered is similar to that considered by McLaren et al. [14].

(a)

(b)   (c)
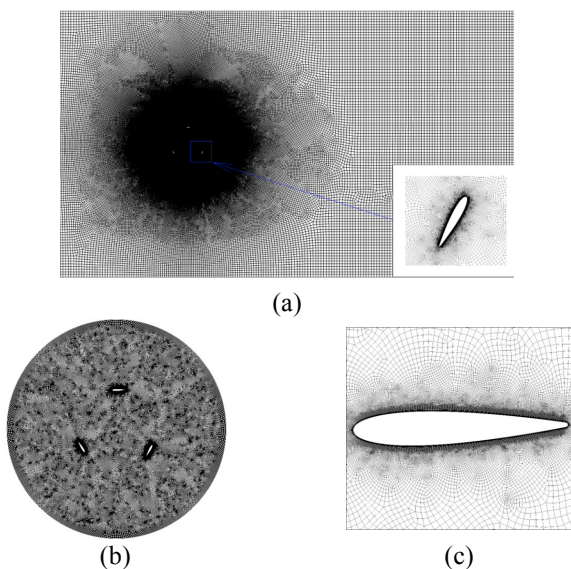
Fig. 2 (a) The meshed computational domain (b) Meshed inner domain (c) Prism layers close to the blade

The domain consists of an inner rotating sub-domain of 7m in diameter (whose larger image is shown in Fig. 1(b)) which houses the turbine blades enclosed in a stationary rectangular outer sub-domain of dimensions 52.5m × 40m. The centre of the rotating domain is placed at a distance of 15m from the inlet of the stationary domain. The connecting arms have not been considered in the analysis and their effect on flow is neglected. The dimensions of the stationary domain have been chosen in such a way that the flow outside the domain is not disturbed due to the presence of the blades. The 2D model is developed using GAMBIT 2.4.6.

2.3 Mesh generation

An unstructured grid graded mesh has been employed in the rotating sub-domain such that the mesh is very fine close to the blades to capture the boundary layer effects and increased in size as it progressed towards the interface as shown in Fig 2. Meshing has been done using ANSYS Workbench. A uniform coarse mesh is employed for the stationary domain as shown in Fig 2(a). A more refined mesh is employed in the rotating sub-domain as the gradients are expected to be high close to the blades (as seen in Fig 2(b)). In the rotating domain prism layers of 17 levels have been used close to the blades to resolve the gradients. The first layer used was of thickness 0.04 mm. This is shown in Fig. 2(c).

2.4 Initial and boundary conditions

The boundaries specified in the problem have been identified in Fig 1(a). For the 2D model, the free stream wind velocity is specified at the inlet with a turbulence intensity of 1%. At the outlet, the pressure is specified to be atmospheric. The blades are specified to be walls with no slip condition. The initial conditions in the whole domain have been assumed to be same as the inlet conditions.

(a)

(b)   (c)
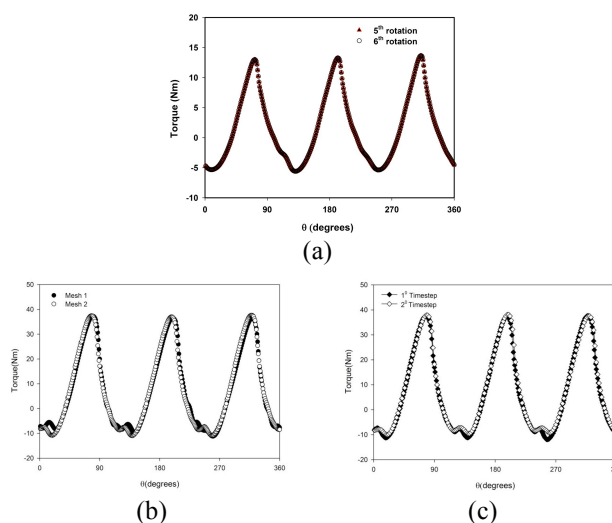
Fig. 3 (a) Torque for consecutive rotations (b) Mesh Independence (c) Time step Independence

2.5 Solution methodology

The solution of the equations is obtained using a commercial CFD coupled solver ANSYS CFX 13.0. The simulations have been done by allowing the rotating domain to rotate at a constant angular velocity decided based on the operating λ. The URANS equations are solved using high-resolution scheme for convection and second-order Euler backward scheme for temporal discretization. The simulations are done until the flow becomes periodic. This has been verified by plotting the average torque produced against azimuthal angle as shown in Fig. 3(a). It can be seen that due to the periodic nature of the flow, the torque obtained from fifth and sixth rotations are similar. In all the

considered cases the flows tend to be periodic after the fifth rotations of the turbine. Thus all characteristics presented in this study are for the sixth rotation of the turbine. The azimuthal angle, θ is the angle made by connecting arm of blade 3 with the vertical axis in anti clockwise direction. The initial position of blade 3 is taken to be $\theta = 0^o$. One full rotation of blade 3 corresponds to $\theta = 0^o$ to 360°.

2.6 Mesh and time step independence

In order to ensure that the numerical solution is independent of the mesh size, simulations have been done using two meshes, a fine mesh (Mesh 1 with 381306 cells) and a coarse mesh (Mesh 2 with 157025 cells). The torque on the turbine shaft is used to compare the dependence of solution on mesh size. The torque variation with azimuthal angle after the flow becomes periodic for Mesh1 and Mesh 2 is shown in Fig. 3(b). It can be observed that the torque obtained from the two different meshes is similar and that the mesh size does not influence the results. Thus Mesh 2 has been used for further simulations due to its lower computational time and good accuracy.

To verify the dependence of solutions on the time step used, simulations were done using Mesh 2 for two different time steps based on the specified speed of the turbine: time required to rotate (1) by one degree, and (2) by two degrees. The variation of torque against θ for both the time steps is shown in Fig 3(c) and it can be seen that the solution becomes time step independent with the time steps used. Thus all the simulations have been done using the following methodology. Initially a 2° time step is used to simulate the first four rotations of the turbine and further rotations are done using 1° time step.

2.7 Validation

The work reported by McLaren et al. [14] has been chosen for the validation of model and solution methodology. They numerically simulated the flow over a small scale high solidity (=0.48) H type three bladed Darrieus VAWT of length 3 m and radius 1.25 m. The blade is of symmetric NACA 0015 profile with a chord length of 0.4 m. The URANS equations with hybrid SST k-ε turbulence model were solved in a 2D computational domain with rotating and stationary sub domains with a sliding mesh interface using CFX. The results were validated against experimental data. The simulations were done for a constant wind velocity of 13.45 m/s over a range of tip speed ratios.

The simulations done by McLaren et al. have been redone using the methodology described in the previous section. C_p is plotted against λ as shown in Fig. 4. The numerical predictions have been compared with the experimental and numerical results reported by McLaren et al. It can be seen that the current values under predicts the experimental values up to about $\lambda = 1.6$ with less deviation.
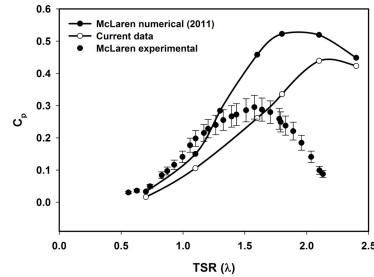
Fig. 4 Validation against McLaren et al. [14]

At higher TSR ($\lambda > 1.6$) the numerical predictions over predict the experimental values. This is also seen with the numerical predictions of McLaren et al. Both the numerical results show similar trends though they vary significantly. At high values of λ, the large deviations observed can be attributed to the 3D effects and the strong wake vortex blade interaction which cannot be predicted with a 2D analysis and the turbulence model considered.

(a)

(b)

(c)
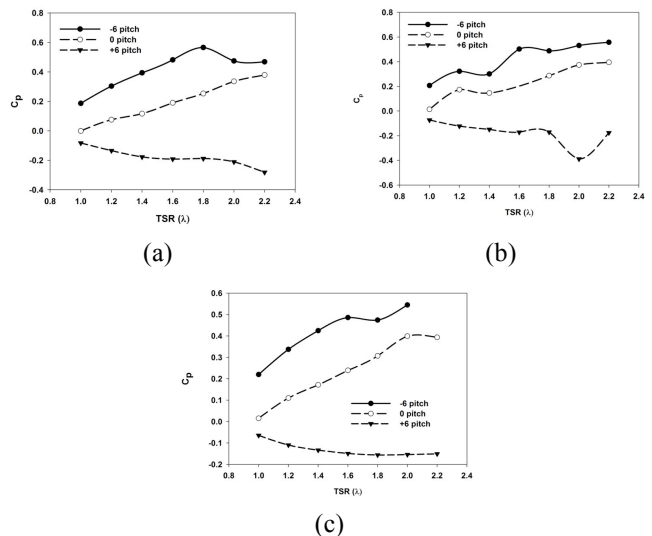
Fig. 5 C_p against λ for U_∞ of (a) 6m/s, (b) 8m/s, (c) 10m/s

3. Results and Discussion

3.1 Effect of pitch angle on performance

In the current study, the analysis has been carried out for β = -6°, 0°,+6° , λ = 1, 1.2, 1.4, 1.6, 1.8, 2, 2.2 and for U_∞ = 6, 8 10 m/s. Figure 5 shows the variation of C_p with λ for different β at U_∞. In this section, the results of the pitch analysis for U_∞ = 6 m/s only is presented. It can be seen similar observations can be made for 8 m/s and 10 m/s from Fig. 5(b) and (c). It can be seen from Fig. 5 that when β = +6°, the C_p values are negative. This is due to the negative torque produced by the blade over one full rotation, meaning
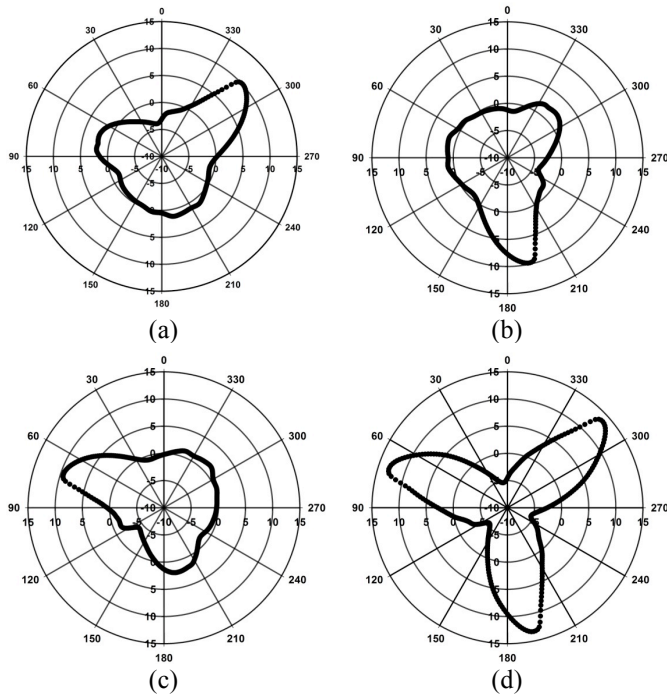
Fig. 6 Polar Charts of variation of torque (Nm) against azimuthal angle (degrees) for λ=1.2, $\beta = 0^o$ and U_∞=6 m/s for (a) blade1 (b) blade 2 (c) blade 3 (d) total torque

that power has to be supplied to the turbine in order to rotate it at the specified angular velocity and hence is not suitable for turbine operation. This effect is more significant at higherλ. At β=0°, the C_p increases with λ.
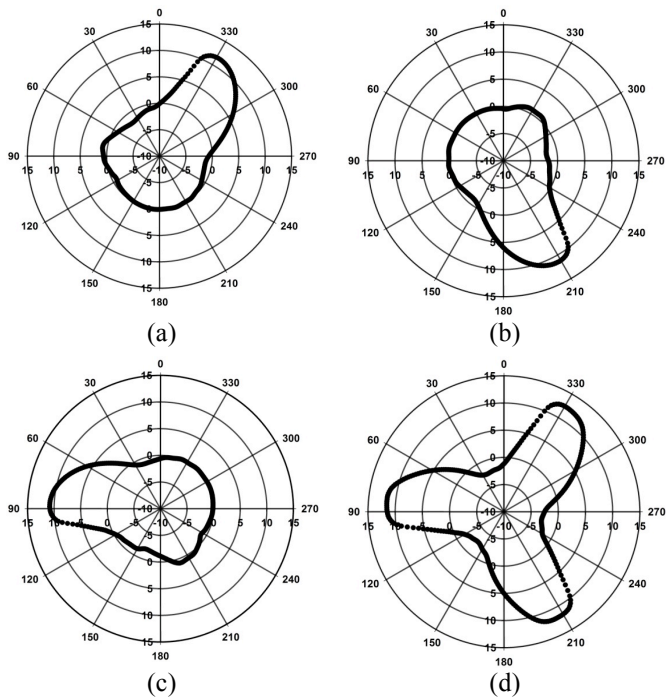
Fig. 7 Polar Charts of variation of torque against azimuthal angle for λ=1.6, $\beta = 0^o$ and U_∞=6 m/s (a) blade1 (b) blade 2 (c) blade 3 (d) total torque

The positive values of C_p mean that the turbine generates power unlike $\beta = +6^o$. At $\lambda = 1$, the net power produced by

the turbine is zero. This behaviour is investigated in the subsequent sections. At $\beta = -6^o$, the C_p increases with increase in λ till 1.8 and then decreases. The maximum C_p is observed at λ=1.8. The performance at $\beta = -6^o$ is better than all other pitch angles at all λ. This is in line with the results reported by Fiedler et al. [4]. To understand this behaviour, the torque characteristics of the blades are looked into.

From Fig. 6 (a) to (c), it can be seen that the individual blade torque curves are similar but have a phase difference, since the blades themselves are angularly offset and have a phase difference. Thus, maximum torque is observed at different azimuthal position for different blades. Form Fig. 6(c), it can be seen that for blade 3 the maximum torque is obtained close to 70° when the blade is in the upwind region where it meets the incident wind directly.
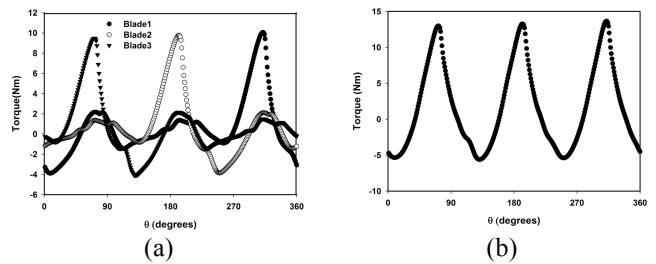
Fig. 8 Linear plot of torque against azimuthal angle for (a) individual blades (b) all blades for $\lambda = 1.2$, $\beta = 0^o$, $U_\infty = 6$ m/s
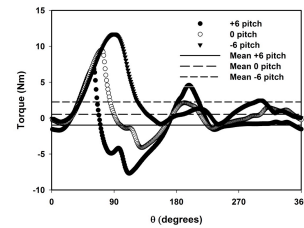
Fig. 9 Torque (blade 3) against θ for different pitch angles for $\lambda = 1.2$ and $U_\infty = 6$ m/s

A closer look will show that for other two blades also, blade torque is high when the blade is in the upwind region. Figure 6(d) shows the total torque against θ (sum of individual blade torques). It can be seen that this curve is also periodic with the peaks occurring at the exact location where peaks occur for individual blades. Thus it can be seen that at any given instant, not all blades contribute to the positive torque. The blade in the upwind region contributes significantly to the positive torque while the other blades either contributes minimally or negate the torque. This explains the observation made in the previous section where the net power is zero for $\beta = 0^o$, λ=1, and U_∞=6 m/s as seen in Fig. 6(a). Figure 7 shows the polar variation of torque against azimuthal angle at λ =1.6, $\beta = 0^o$ and $U_\infty = 6$m/s. The behaviour is similar to that seen for λ =1.2. It can also be seen that with the increase in λ, the location of maximum torque and the band of the torque curve increases meaning that the blade experiences higher torque and also for a wider range of azimuthal angle. This

behaviour can also be inferred from the linear plot of torque against azimuthal angle for $\lambda = 1.2$, $\beta = 0^o$, $U_\infty = 6$ m/s. (Fig 8(a) & (b)). Based on the observations made above, it can be concluded that an analysis of the torque characteristics of the

upwind blade is sufficient to understand the torque characteristics of the turbine and hence the effect of pitch angle on the performance of the turbine.
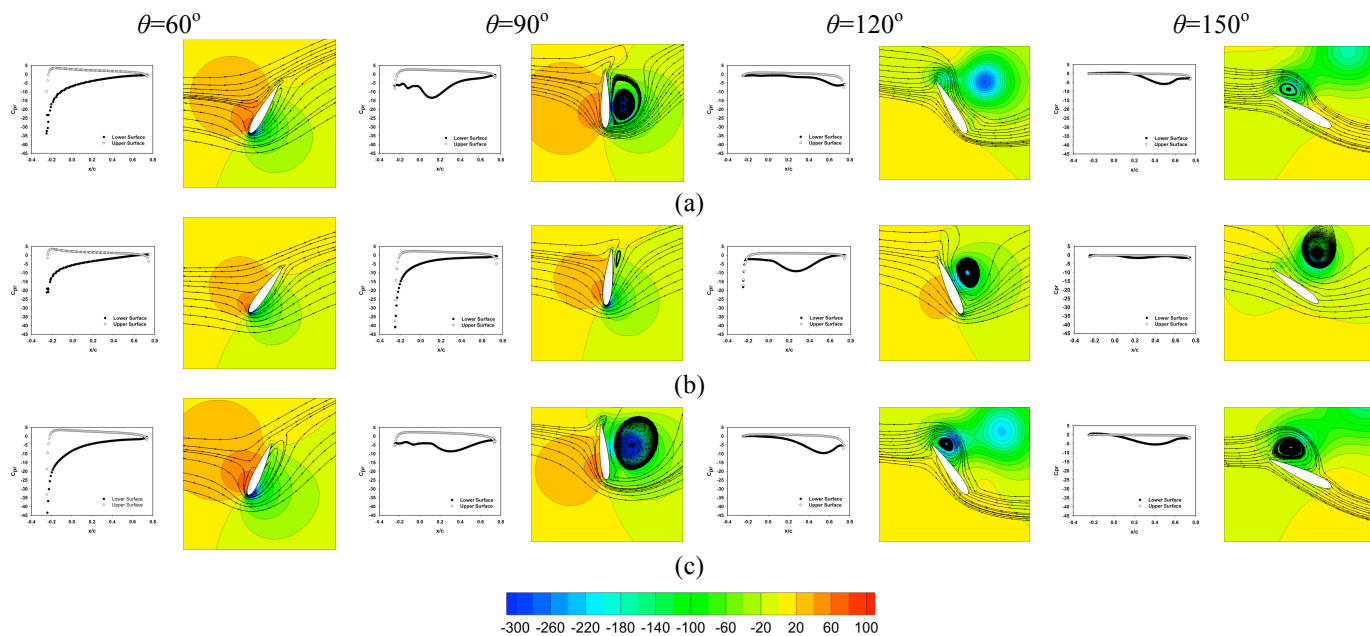
Fig. 10 C_{pr} variation along the blade surface and corresponding pressure contours (Pa) with stream lines for for $\lambda = 1.2$ and U_∞ = 6 m/s (a) $\beta = 0^o$, (b) $\beta = - 6^o$, (c) $\beta = + 6^o$

The torque acting on blade 3 (which is in the upstream position for $\theta = 0^o$ to 180°) for different pitch angles for $\lambda = 1.2$ and $U_\infty = 6$ m/s is shown in Fig. 9. It can be seen that the peak increases in value shifts to higher azimuthal angles for negative pitch angle. It can also be seen that the band of the curve for which the torque is positive increases for negative pitch. For $\beta = 6^o$, the torque is negative for a significant range of θ and this is not seen with $\beta = -6^o$. To investigate this behaviour, the forces acting on the blades, which are responsible for the torque on the blades, are looked into. When air flows past the blade, the forces acting on the blade are due to the pressure difference across the upper and lower surfaces of the blade and the shear force, due to the viscosity and velocity gradients of air. Since the viscosity of air is very low, the shear force is found to be negligible in comparison to the pressure force. Hence, the torque on the blades can be attributed to the forces due to differential pressure across the blades. To understand the effect of pressure on the blade surfaces on the torque produced by the blade, a non-dimensional parameter called coefficient of pressure ($C_{pr} = (p - p_\infty)/(0.5\rho U_\infty^2)$) is used. A positive value of C_{pr} implies the pressure is higher than the atmospheric pressure p_∞. Figures 10 show the variation of C_{pr} along the upper (unfilled) and lower surfaces (filled) of the blade profile of blade 3 and the pressure contours with the streamlines near blade 3 at different azimuthal positions ($\theta = 60^o$ to 150°) for of blade 3 for $\beta = 0^o, -6^o$ and $+6^o$.

Figure 10(a) shows pressure coefficient variation and pressure contours for $\beta = 0^o$. At $\theta = 60^o$, the area enclosed is high near the leading edge implying a high pressure difference across the blade surfaces and consequently high torque as seen in Fig 9. The flow remains attached to the blade and streamlined over the blade. At $\theta = 90^o$, the region enclosed by the C_{pr} curve is almost constant over the entire length. The stream lines show a large recirculation formed on the bottom surface of the blade. This results in a relatively lower positive torque as seen from Fig. 9. At $\theta = 120^o$ and 150°, area enclosed by the C_{pr} is relatively small with larger bands close to the trailing end. This is due to the blade becoming more in line with the incident wind with increase in azimuthal angle. From the stream lines the presence of vortices close to the trailing edge can be seen. The small vortex at 120° is seen to have increased in strength at 150°. As pointed out the large pressure difference observed close to the trailing edge of the blade with increase in θ causes these vortices. This decreases the positive torque acting on the shaft. This can be observed from Fig. 9 where large negative torque is seen at $\theta = 120^o$ and 150°. Thus, larger area enclosed by the C_{pr} curve represents larger pressure difference across the upper and lower surfaces of the blade and hence, larger would be the lift force acting on the blade. It is observed that a larger area enclosed close to the leading edge results in higher lift forces and thus high torque on the shaft whereas when observed close to the trailing edge leads to negative effect due to flow separation. With increase in θ, the area enclosed also increases till it reaches a peak value

and then starts declining with θ. This is the same trend seen for total torque with θ. The torque is maximum near 60° for this case and the area enclosed by the C_{pr} curve close to the leading edge is also the largest at 60° as seen in Fig. 10 (a). This similarity is observed at 90° and 60° for β = -6° (Fig. 10 (b)) and β = +6° (Fig. 10 (c)) respectively.

Observations made from Fig 10(a) can be seen in Fig. 10(b) and 10(c). The flow is attached to the blade surface enabling the blade surface to produce lift at lower values of θ (<90°). With increase in θ, flow separates near the trailing edge leading to low lift and hence low torque. As the blades are in line with the flow, the blades experience more drag than lift and hence low torque. Also, the torque produced is very low or negative when vortices occur in the flow. This is because a significant amount of the kinetic energy of the incident wind is converted to the kinetic energy of the vortices and is not transferred to the blades. For β= -6° as seen from Fig. 10(b), the flow remains streamlined for a longer period and thus positive torque is obtained for larger range of θ as pointed out from Fig. 9. It can be seen from the stream lines at θ=120° (Fig. 10 (b)), the trailing vortex seen with zero pitch case is absent. At θ=150° (Fig. 10 (b)) a small weak trailing vortex initiation is observed. Due to toe out configuration of the blade, flow remains stream lined for a larger range of θ. For β=+6° as seen in Fig. 10(c), the trailing vortices initiate at earlier θ =90° (Fig. 10(c)) and they grow to become stronger vortices as compared to other pitches as seen in Fig 10 (c). Thus the torque is highest for β = -6° followed by β = 0° and β = +6° as seen in Fig. 9.

4. Conclusions

The effect of pitch angle on the performance of a three bladed straight H-Darrieus VAWT was studied numerically using a commercial CFD code. The simulations were done using a 2D model with SST k-ε turbulence model for β = -6°, 0°, +6°, different λ and U_∞ of 6, 8 and 10 m/s. The following conclusions have been drawn from the study.

1. Of the three pitches considered, the negative pitch was found to give the best performance over the entire range of TSR and at all wind velocities.

2. The pressure coefficient plots over the upwind blade surface and streamlines showed that the presence of vortices close to the trailing edge deteriorates the performance of the turbine. Thus, to improve the performance of the turbine, the initiation of such vortices need to be delayed in the upwind region. One strategy seen is the use to toe out pitch which delays the trailing edge vortex improving the performance of the turbine.

3. From the benchmark studied, it was understood that 3D CFD analysis is required for more realistic predictions especially at high TSRs. Three dimensional analysis is required to take into account the end effects and strong interaction between the trailing vortices and the following blade.

References

[1] Aslam Bhutta, M.M., N. Hayat, A.U. Farooq, Z. Ali, S.R. Jamil, and Z. Hussain, Vertical axis wind turbine–A review of various configurations and design techniques. Renewable and Sustainable Energy Reviews, 2012. 16(4): p. 1926-1939.

[2] Lazauskas, L., Three pitch control systems for vertical axis wind turbines compared. Wind Engineering, 1992. 16(5): p. 269-282.

[3] Miau, J.J., S.Y. Liang, R.M. Yu, C.C. Hu, T.S. Leu, J.C. Cheng, and S.J. Chen, Design and Test of a Vertical-Axis Wind Turbine with Pitch Control. Applied Mechanics and Materials, 2012. 225: p. 338-343.

[4] Fiedler, A.J. and S. Tullis, Blade offset and pitch effects on a high solidity vertical axis wind turbine. Wind Engineering, 2009. 33(3): p. 237-246.

[5] Klimas, P.C., Darrieus rotor aerodynamics. ASME, Transactions, Journal of Solar Energy Engineering, 1982. 104: p. 102-105.

[6] Nobile, R., M. Vahdati, J. Barlow, and A. Mewburn-Crook, Dynamic stall for a vertical axis wind turbine in a two-dimensional study. World Renew. Energ. Congr, 2011: p. 4225-4232.

[7] Qin, N., R. Howell, N. Durrani, K. Hamada, and T. Smith, Unsteady flow simulation and dynamic stall behaviour of vertical axis wind turbine blades. Wind Engineering, 2011. 35(4): p. 511-528.

[8] Chen, C.-C. and C.-H. Kuo, Effects of pitch angle and blade camber on flow characteristics and performance of small-size Darrieus VAWT. Journal of Visualization, 2013. 16(1): p. 65-74.

[9] Howell, R., N. Qin, J. Edwards, and N. Durrani, Wind tunnel and numerical study of a small vertical axis wind turbine. Renewable Energy, 2010. 35(2): p. 412-422.

[10] Erickson, D.W., J.J. Wallace, and J. Peraire, Performance Characterization of Cyclic Blade Pitch Variation on a Vertical Axis Wind Turbine. 2011.

[11] Sabaeifard, P., H. Razzaghi, and A. Forouzandeh. Determination of Vertical Axis Wind Turbines Optimal Configuration through CFD Simulations.

[12] Benedict, M., V. Lakshminarayan, J. Pino, and I. Chopra, Fundamental Understanding of the Physics of a Small-Scale Vertical Axis Wind Turbine with Dynamic Blade Pitching: An Experimental and Computational Approach. 2013.

[13] ANSYS CFX Solver Theory Guide 13.0. 2010, ANSYS Inc.

[14] McLaren, K., S. Tullis, and S. Ziada, Computational fluid dynamics simulation of the aerodynamics of a high solidity, small-scale vertical axis wind turbine. Wind Energy, 2012. 15(3): p. 349-361.